Energy Conserving Lattice Boltzmann Models for Incompressible Flow Simulations

Shiwani Singh[1], Siddharth Krithivasan[1], Iliya V. Karlin[2,3], Sauro Succi[4] and Santosh Ansumali[1,*]

[1] *Engineering Mechanics Unit, Jawaharlal Nehru Centre for Advanced Scientific Research, Jakkur, Bangalore 560064, India.*
[2] *Aerothermochemistry and Combustion Systems Lab, ETH Zurich, 8092 Zurich, Switzerland.*
[3] *Energy Technology Research Group, School of Engineering Sciences, University of Southampton, Southampton, SO17 1BJ, UK.*
[4] *Istituto Applicazioni Calcolo "Mauro Picone", C.N.R., Via dei Taurini, 19, 00185, Rome, Italy.*

Abstract. In this paper, we highlight the benefits resulting from imposing energy-conserving equilibria in entropic lattice Boltzmann models for isothermal flows. The advantages are documented through a series of numerical simulations, such as Taylor-Green vortices, cavity flow and flow past a sphere.

AMS subject classifications: 82C40

Key words: Lattice Boltzmann method.

1 Introduction

In the last decade, mesoscale algorithms such as lattice Boltzmann models (LBM), Dissipative Particle Dynamics (DPD) and multi-particle collision dynamics, have attracted increasing interest in the framework of computational fluid dynamics (see, e.g., [1–15]). This success story is remarkable from the theoretical point of view too, as continued effort in this field has succeeded in establishing the existence of a self-consistent underlying micro-dynamics behind the mesoscopic formulation.

Corresponding author. Email addresses: `shiwani@jncasr.ac.in` (S. Singh), `siddharth@jncasr.ac.in` (K. Siddharth), `ilya.karlin@gmail.com`, `karlin@lav.mavt.ethz.ch` (I. V. Karlin), `succi@iac.cnr.it` (S. Succi), `ansumali@jncasr.ac.in` (S. Ansumali)

For example, in the case of LBM, the importance of formulating discrete kinetic models in compliance with the H-theorem, is by now fully appreciated [3, 16–21]. In fact, an exact lattice analog of the continuous Maxwell-Boltzmann distribution was derived from a discrete version of the entropy maximization principle [19,20,22]. The link between discrete thermodynamics and numerical stability and efficiency of the corresponding computational model, is also well appreciated and possible generalizations towards more microscopic formulations have been explored in recent works [11, 19, 23–27].

Despite the aforementioned success of these approaches, much still needs to be understood, both from theoretical and numerical standpoint, such as efficient implementation of curved boundaries, numerical stability at very low viscosity and others.

In the present manuscript, we show that releasing a specific thermodynamic deficiency of the method, leads to a significant improvement in the quality of the simulation. More precisely, in its present popular isothermal setting, sound propagation in lattice Boltzmann [28], takes place at constant temperature, thus following Newton's definition of sound speed,

$$c_s^2 = \frac{\partial P}{\partial \rho}\bigg|_T = \frac{k_B T_0}{m} \equiv v_0^2, \tag{1.1}$$

where v_0 is the reference thermal speed.

However, via Laplace theory, it is known that, in actual reality, sound propagation occurs via an adiabatic process, which can only be described by an energy conserving (EC) model. This automatically gives,

$$c_s^2 = \frac{\partial P}{\partial \rho}\bigg|_S = \gamma \frac{k_B T_0}{m}, \tag{1.2}$$

where γ is the adiabatic exponent. Traditionally, this discrepancy was largely neglected in isothermal LBM simulations, with an argument that the relevant observable is the velocity field, the sound speed being just an immaterial constant. However, as we shall show in the following, this thermodynamic aspect plays a major role in determining the quality of simulation results even for isothermal flows in fully resolved domains. In other words, reproducing the correct sound speed gives rise to a much more robust numerical scheme.

The work is organized as follows. In Section 2, lattice Boltzmann model (both energy conserving and isothermal) is briefly reviewed. In Section 3, via an example we show that energy conserving model indeed manages to reproduce adiabatic sound propagation correctly. In Section 4, we compare the energy conserving model with isothermal model for the set up of Taylor-Green vortex, cavity flow and flow past a sphere. Finally, we summarize results of the study in Section 5.

2   Lattice Boltzmann method

We briefly remind the reader that, in typical LBM formulations, one works with a set of discrete populations $f = \{f_i\}$, corresponding to predefined discrete velocities $\mathbf{c}_i$ ($i =$

$1, \cdots, N$). The hydrodynamic variables, such as the mass density, ρ and the momentum density, ρu_α and temperature T, are defined to be the lowest order moments of the distribution function, namely:

$$\rho = \sum_{i=1}^{N} f_i, \qquad \rho u_\alpha = \sum_{i=1}^{N} f_i c_{i\alpha}, \qquad P \equiv \frac{1}{2}\rho u^2 + \frac{D}{2}\rho \frac{k_B T}{m} = \frac{1}{2}\sum_{i=1}^{N} f_i c_i^2. \tag{2.1}$$

For this set of discrete populations, the evolution equation is often written in the single-time relaxation BGK-form [29], as

$$\frac{df}{dt} = \frac{1}{\tau}[f^{eq}(M^{\text{Slow}}(f)) - f], \tag{2.2}$$

where slow moments are typically taken as $M^{\text{Slow}} = (\rho, \mathbf{u})$ and τ is the smallest time scale of relaxation (related with viscosity), d/dt represents derivative along the discrete characteristics and f^{eq} is a discrete equivalent of the Maxwell-Boltzmann equilibrium, a local functional of the slow moments. The explicit form of this discrete equilibrium is known [19, 20]. In this entropic formulation of the LB method [19, 20], in its most general setting one works with discrete thermodynamic potential

$$H = \sum_{i=1}^{N} \left[f_i \left(\ln\left(\frac{f_i}{w_i}\right) - 1 \right) + \alpha f_i + \beta_\zeta c_{i\zeta} f_i + \gamma c_i^2 f_i \right], \qquad w_i > 0, \tag{2.3}$$

where w_i are the weights associated with the quadrature, α, β_ζ and γ are the Lagrange multipliers associated with the conservation laws; in this setting, f_i^{eq} provides the minimum to the H-function (2.3). The formal expression for the equilibrium distribution reads as follows (This expression is applicable only in 2D and 3D.)

$$f_i^{eq} = w_i \exp\left(\alpha + \beta_\zeta c_{i\zeta} + \gamma c_i^2\right). \tag{2.4}$$

In the special case of isothermal hydrodynamics, energy conservation is ignored and thus one sets $\gamma = 0$. An explicit expression of the equilibrium for $D1Q3$, $D2Q9$ and $D3Q27$ model, reads as follows [19],

$$f_i^{\text{eq}}(\rho, u_\alpha) = \rho w_i \prod_{\alpha=1}^{D} \left[\left(2 - \sqrt{1 + \frac{u_\alpha^2}{\theta_0}} \right) \left\{ \frac{\left(2\frac{u_\alpha}{c} + \sqrt{1 + \frac{u_\alpha^2}{\theta_0}} \right)}{1 - \frac{u_\alpha}{c}} \right\}^{c_{i\alpha}/c} \right], \tag{2.5}$$

where lattice unit $c = \sqrt{3k_B T_0/m}$ which assumes that the dimensionless temperature defined in the lattice units is $\theta_0 = k_B T_0/(mc^2)$ and the exponent $c_{i\alpha}/c$ takes the value ± 1 and 0 only (i refers to discrete velocity and α refers to direction). However, in practice, a polynomial approximation to the exact equilibria, is often used,

$$f_i^{\text{eq}} = w_i \rho \left[1 + \frac{u_\alpha c_{i\alpha}}{c^2 \theta_0} + \frac{u_\alpha u_\beta}{2c^4 \theta_0^2}\left(c_{i\alpha} c_{i\beta} - \theta_0 c^2 \delta_{\alpha\beta}\right) \right], \tag{2.6}$$

with weights in D dimensions as

$$w_i = (1-\theta_0)^D \left(\frac{\theta_0}{2(1-\theta_0)}\right)^{(c_i/c)^2}. \tag{2.7}$$

In the case of energy conserving hydrodynamics, the explicit form of the resulting equilibrium distribution can be found, for $u=0$, as a function of reduced temperature $\theta = k_B T/(mc^2)$ measured in lattice unit and is given as

$$f_i^{\mathrm{eq}} \equiv \rho W_i(\theta) = \rho(1-\theta)^D \left(\frac{\theta}{2(1-\theta)}\right)^{(c_i/c)^2}. \tag{2.8}$$

For non-zero velocity case, perturbative equilibria is found to take the following form [20],

$$f_i^{\mathrm{eq}} = \rho W_i(\theta) \left[1 + \frac{u_\alpha c_{i\alpha}}{c^2\theta} + \frac{u_\alpha u_\beta}{2c^2\theta^2}\left(\frac{c_{i\alpha}c_{i\beta}}{c^2} - \frac{2D\theta^2 + 3(c_i/c)^2(\theta_0-\theta)}{D(3\theta_0-\theta)}\delta_{\alpha\beta}\right)\right] + \mathcal{O}(u^3), \tag{2.9}$$

where θ is the dimensionless temperature and the isothermal equilibrium is recovered in the limit $\theta \to 1/3$. The expression given above is applicable only for 2D and 3D, as for $D1Q3$ model it is not possible to impose energy conservation. The lattice Boltzmann models with multiple relaxation time (not in the scope of present study) have different stability behavior in comparison to single relaxation time model [30].

In Lattice Boltzmann equation, the trapezoidal discretization of the underlying PDE is used, to obtain,

$$f(x+\mathbf{c}\Delta t, t+\Delta t) = f(x,t) + 2\beta \left[f^{eq}(M^{\mathrm{Slow}}(x,t)) - f(x,t)\right]. \tag{2.10}$$

In the above equation, the discrete dimensionless relaxation parameter, $\beta = \Delta t/(2\tau + \Delta t)$, dictates the stability domain of the method.

3 Sound propagation in energy conserving model

The first implication of using the energy conserving model is that the sound speed takes on its correct, isentropic, value. In order to show that this is indeed the case, we performed a simulation using the D2Q9 model with the following initial conditions:

$$\rho(x,y,t=0) = 1 + \epsilon \cos(kx), \qquad \theta(x,y,t=0) = \frac{\rho}{3}, \qquad u_x = u_y = 0.0. \tag{3.1}$$

Here, ϵ is a small amplitude of a periodic density perturbation which allows us to observe the acoustic mode [31]. As the ratio of specific heat capacity $\gamma = (D+2)/2 = 2$ in the two-dimensional case, we expect the ratio of the sound speed measured from energy
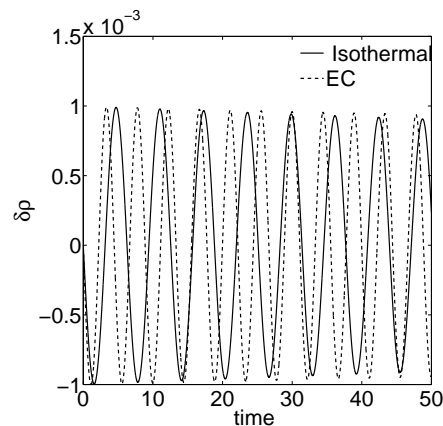
Figure 1: Variation of density with time in LB simulation at the center of domain for Re$=50$, Ma$=0.1$ and grid-size $=700\times700$.

conserving and isothermal lattice Boltzmann to be $\sqrt{2}$. As shown in the Fig. 1, the ratio between the speed of sound for energy conserving with that of isothermal is indeed $\approx$ 1.414. As can be seen from the figure, energy conserving model has 11 crests and 12 troughs, so the value is in between 11 and 12 ($\approx$ 11.25), while isothermal model has 8 crests and 8 troughs. So the ratio is $11.25/8\approx1.406$

4 Results

4.1 Taylor-Green vortex and convergence of lattice Boltzmann

In order to illustrate the benefits of energy conserving model over isothermal model, as the next example, we consider the Taylor-Green vortex, for which an analytical solution for 2-D incompressible Navier-Stokes equation is available. The initial condition is,

$$u_x(x,y,t=0) = U_0\sin\left(\frac{2\pi}{L}k_x x\right)\cos\left(\frac{2\pi}{L}k_y y\right), \tag{4.1a}$$

$$u_y(x,y,t=0) = -\frac{k_x}{k_y}U_0\cos\left(\frac{2\pi}{L}k_x x\right)\sin\left(\frac{2\pi}{L}k_y y\right). \tag{4.1b}$$

The initial condition on density and temperature θ is

$$\rho(x,y,t=0)=1, \qquad \theta(x,y,t=0)=1/3. \tag{4.2}$$

The advantage of this set-up is that the error analysis directly reveals the different accuracy of the isothermal and energy conserving methods, in the absence of boundary effects. We performed a grid resolution study using the L_1 and L_2 error norms (calculated with respect to analytical solution) of the velocity in x direction for a given Mach
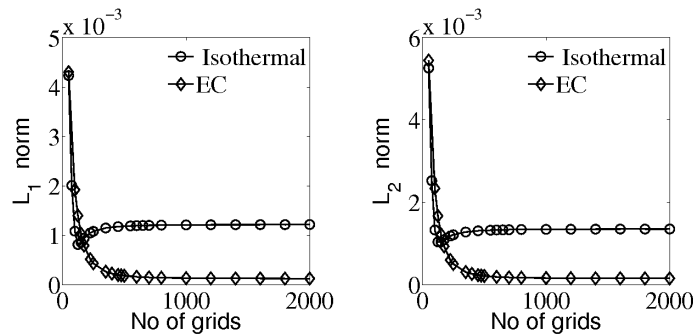
Figure 2: L_1 and L_2 norm for velocity in x direction at Re$=250$ and Ma$=0.05$ for Taylor-Green vortex with different grid size.
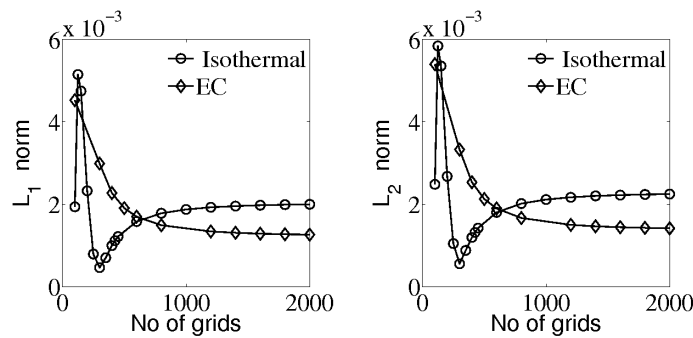

Figure 3: L_1 and L_2 norm for velocity in x direction at Re$=4000$ and Ma$=0.05$ for Taylor-Green vortex with different grid size.

(Ma) and Reynolds numbers (Re). Here, Re is based on the characteristic length of the flow-field, taken as 2π in a periodic-box of length 2π, thus $=U_0 2\pi/\nu$. Results are demonstrated in Figs. 2 and 3. We have defined the computational Mach number as Ma$=U_0/v_0$. Notice that for the energy conserving model, the effective Mach number is lower by a factor of $\sqrt{\gamma}$. We have chosen this definition for comparing two methods, as this computational Mach number is the one which gives the idea about computational cost. In other words, for same computational cost, the effective Mach number is lower than in energy conserving model.

It is evident from the figures that, at Re$=250$, the error in the energy-conserving case is an order of magnitude smaller than in the isothermal case. Even more importantly, the error does not show any sign of decay beyond $N \sim 200$. The case Re$=4000$ conveys essentially the same message, although it is to be noted that at low resolution, the isothermal model may even lead to a smaller error than the energy-conserving one. However, as resolution is increased, the error saturates, while the energy-conserving models show a progressive, if only slow, decay. It can be seen from Figs. 2 and 3, that isothermal model shows oscillatory convergence while energy conserving model shows uniform convergence. It can also be inferred from the figures that incidentally at low resolution

($N\sim200$), isothermal model gives smaller error than energy conserving model. However, as resolution is increased, energy conserving model becomes slightly more accurate.

In Table 1, error vs wavenumber for Taylor-Green flow simulation at Ma $=0.05$ and Re $=250$ is presented.

Table 1: Error as a function of wavenumber.

Grid	Δx	$\frac{\Delta t}{\tau}$	$\Delta k c_s \tau$	$L_{1(\mathrm{iso})}/L_{1(\mathrm{EC})}$
250	0.025120	11.54730	0.049998	2.49655108559788898662
450	0.0139556	6.415188	0.089997	5.94319296790443147449
600	0.01048	4.8175	0.11984	7.51231356662535934226
1000	0.0062857	2.889445	0.1998135	9.11464142525547885328
1200	0.005238	2.407833	0.2397800	9.39975804200142693178
2000	0.003142	1.44433	0.3997351	9.80366544915056078308
3000	0.0020933	0.9617607	0.60000955	9.92481386947622503649

4.2 Cavity flow

In actual practice, many fluid dynamic simulations take place in wall-bounded domains. Therefore, in our next example, we consider 2D lid driven cavity, for which the polynomial-based isothermal LBM is known to produce unstable solutions at low grid resolution. The parameters used in simulation are Re $=5000$, Ma $=0.1732$ and both isothermal (polynomial based) as well as energy-conserving simulations were performed with different grid sizes, with diffusive wall boundary conditions. From Figs. 4-6, it can be seen that the energy-conserving setup converges towards a steady state value at a lower grid size than the isothermal.

In this setup, which is a prototype for bounded flows, we observed that the differences between the two models were more pronounced. In order to show this effect, in Tables 2 and 3 the percentage error in stream function value at center vortex for Re$=5000$ and Ma($=0.05$ and 0.087) with different grid size is shown. The converged value for comparison is taken from [32].

Table 2: Percentage error in stream function value at center vortex at Ma $=0.05$ and Re $=5000$.

Grid Points	200	256	312	375	450
Isothermal	17.92	6.067	3.616	2.328	2.148
EC	7.36	4.977	3.64	2.73	2.29

Table 3: Percentage error in stream function value at center vortex at Ma $=0.087$ and Re $=5000$.

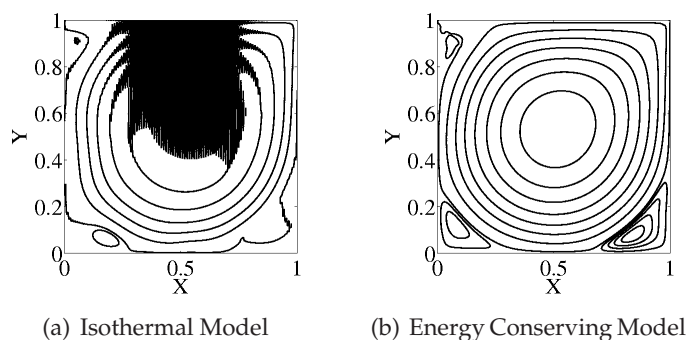| Grid Points	200	256	312	375	450	512
Isothermal	30.88	5.067	3.1484	2.312	1.908	1.721
EC	5.223	3.903	2.837	2.017	1.509	1.369

(a) Isothermal Model   (b) Energy Conserving Model

Figure 4: Streamline plot of cavity flow for grid-size=200×200. The isothermal model (left) is patently unstable, while the energy-conserving one (right) shows no sign of instability.
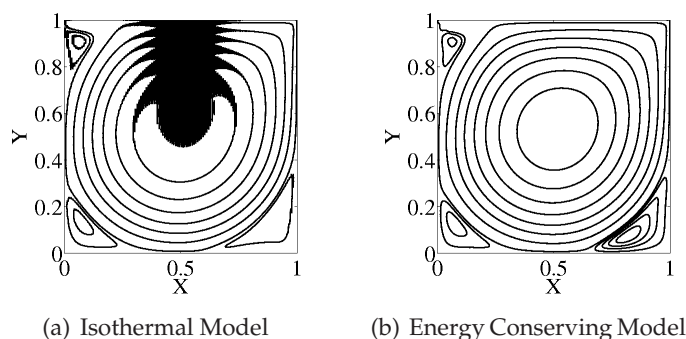

(a) Isothermal Model   (b) Energy Conserving Model

Figure 5: Streamline plot of cavity flow for grid-size=256×256. The isothermal model is still unstable, although to a less extent than for the case 200×200. The energy-conserving one shows also a small improvement over the 200×200, especially around the top-left corner.
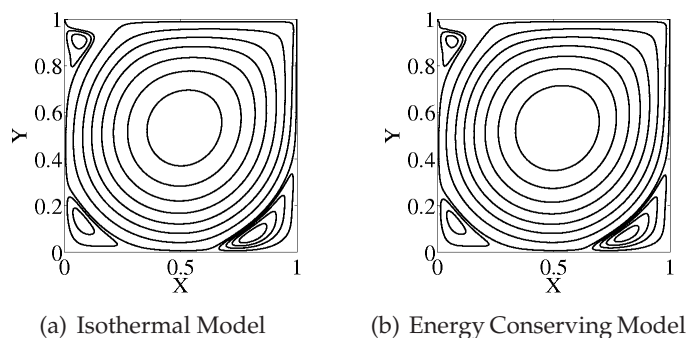

(a) Isothermal Model   (b) Energy Conserving Model

Figure 6: Streamline plot of cavity flow for grid-size=312×312.

We can see that the energy conserving model is more effective in suppressing acoustic disturbances arising near boundaries. In order to verify that indeed this is the case, in next section flow past a sphere is reported.

4.3 Flow past a sphere

As our final example, we consider the LB application in complex geometry, and notably a 3D simulation of flow around the sphere, with Re$=118$, Ma$=0.104$, the radius of the sphere being 10 lattice units.

The initial density and the temperature are chosen as $\rho=1.0$ and $\theta=1/3$ respectively. A Grad type boundary condition [33] is used for the inlet and outlet. Free-slip boundary condition is used for top and bottom boundaries and periodic boundary condition is used for the other direction.

From Fig. 7, it is clearly visible that the isothermal LB fails to capture the pressure profile, especially at inlet and outlet regions, while the energy-conserving one does not show any problem. On the other hand, both methods succeed in capturing the velocity profile to a satisfactory degree of accuracy.
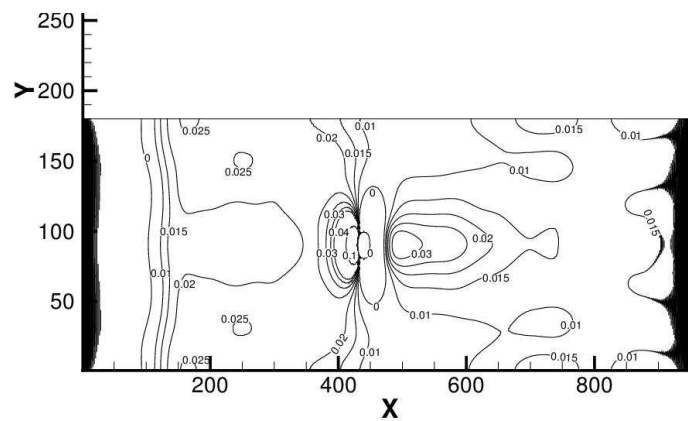
(a) Isothermal Model
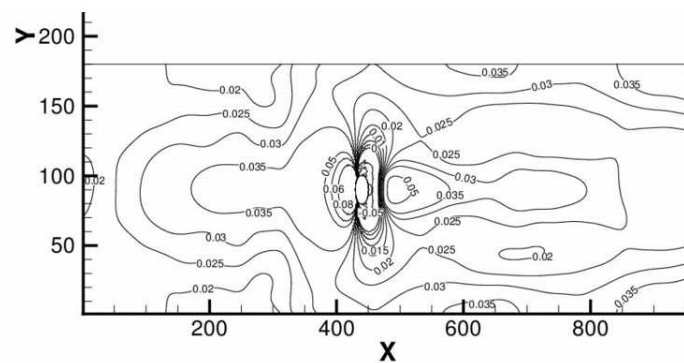
(b) Energy Conserving Model

Figure 7: Pressure contour plot of flow around sphere for grid-size$=960\times180\times180$.

5   Outlook

Summarizing, we have shown that the accuracy and robustness of the isothermal LB method show significant improvement upon incorporating the energy-conservation constraint, securing the correct sound speed.

Acknowledgments

References

[1] S. Chen and G.D. Doolen. Lattice Boltzmann method for fluid flows. Annual Review of Fluid Mechanics, 30(1):329, 2003.

[2] C.K. Aidun and J.R. Clausen. Lattice-Boltzmann method for complex flows. Annual Review of Fluid Mechanics, 42:439–472, 2010.

[3] S. Succi, I.V. Karlin, and H. Chen. Colloquium: Role of the H theorem in lattice Boltzmann hydrodynamic simulations. Reviews of Modern Physics, 74(4):1203–1220, 2002.

[4] F.J. Higuera and J. Jimenez. Boltzmann approach to lattice gas simulations. EPL (Europhysics Letters), 9:663, 1989.

[5] S. Succi. The lattice Boltzmann equation for fluid dynamics and beyond. Oxford University Press, USA, 2001.

[6] P. Espanol and P. Warren. Statistical mechanics of dissipative particle dynamics. EPL (Europhysics Letters), 30:191, 1995.

[7] R.D. Groot and P.B. Warren. Dissipative particle dynamics: Bridging the gap between atomistic and mesoscopic simulation. Journal of Chemical Physics, 107(11):4423, 1997.

[8] A. Malevanets and R. Kapral. Mesoscopic model for solvent dynamics. Journal of Chemical Physics, 110(17), 1999.

[9] R.D. Groot and K.L. Rabone. Mesoscopic simulation of cell membrane damage, morphology change and rupture by nonionic surfactants. Biophysical Journal, 81(2):725–736, 2001.

[10] H. Noguchi and G. Gompper. Swinging and tumbling of fluid vesicles in shear flow. Physical review letters, 98(12):128103, 2007.

[11] S. Ansumali, I.V. Karlin, S. Arcidiacono, A. Abbas, and N.I. Prasianakis. Hydrodynamics beyond Navier-Stokes: Exact solution to the Lattice Boltzmann hierarchy. Physical review letters, 98(12):124502, 2007.

[12] H. Chen, S. Kandasamy, S. Orszag, R. Shock, S. Succi, and V. Yakhot. Extended Boltzmann kinetic equation for turbulent flows. Science, 301(5633):633, 2003.

[13] R.D. Groot and T.J. Madden. Dynamic simulation of diblock copolymer microphase separation. The Journal of chemical physics, 108:8713, 1998.

[14] R. Benzi, S. Succi, and M. Vergassola. The lattice Boltzmann equation: theory and applications. Physics Reports, 222(3):145–197, 1992.

[15] F.J. Higuera, S. Succi, and R. Benzi. Lattice gas dynamics with enhanced collisions. EPL (Europhysics Letters), 9:345, 1989.

[16] I. V. Karlin, A. Ferrante, and H. C. Öttinger. Perfect entropy functions of the lattice Boltzmann method. Europhys. Lett., 47:182–188, 1999.

[17] A.J. Wagner. An H-theorem for the lattice Boltzmann approach to hydrodynamics. EPL (Europhysics Letters), 44:144, 1998.

[18] B.M. Boghosian, P.J. Love, P.V. Coveney, I.V. Karlin, S. Succi, and J. Yepez. Galilean-invariant lattice-Boltzmann models with H theorem. Physical Review E, 68(2):025103, 2003.

[19] S. Ansumali, I. V. Karlin, and H. C. Öttinger. Minimal entropic kinetic models for simulating hydrodynamics. Europhys. Lett., 63:798–804, 2003.

[20] S. Ansumali and I.V. Karlin. Consistent Lattice Boltzmann method. Physical review letters, 95(26):260605, 2005.

[21] I. V. Karlin, S. Succi, and S. S. Chikatamarla. Comment on "numerics of the lattice boltzmann method: Effects of collision models on the lattice boltzmann simulations". Phys. Rev. E, 84:068701, Dec 2011.

[22] P. Asinari and I.V. Karlin. Generalized Maxwell state and H-theorem for the lattice Boltzmann method. Phys. Rev. E, 79(3):36703, 2009.

[23] S.S. Chikatamarla and I.V. Karlin. Entropy and Galilean invariance of lattice Boltzmann theories. Physical review letters, 97(19):190601, 2006.

[24] X.B. Nie, X. Shan, and H. Chen. Galilean invariance of lattice Boltzmann models. EPL (Europhysics Letters), 81:34005, 2008.

[25] L. Szalmás. Knudsen layer theory for high-order lattice Boltzmann models. EPL (Europhysics Letters), 80:24003, 2007.

[26] X. Shan. General solution of lattices for Cartesian lattice Bhatanagar-Gross-Krook models. Physical Review E, 81(3):036702, 2010.

[27] W.P. Yudistiawan, S.K. Kwak, D.V. Patil, and S. Ansumali. Higher-order Galilean-invariant lattice Boltzmann model for microflows: Single-component gas. Physical Review E, 82(4):046701, 2010.

[28] R.R. Nourgaliev, T.N. Dinh, T.G. Theofanous, and D. Joseph. The lattice Boltzmann equation method: theoretical interpretation, numerics and implications. International Journal of Multiphase Flow, 29(1):117–169, 2003.

[29] P. L. Bhatnagar, E. P. Gross, and M. Krook. A Model for Collision Processes in Gases. I. Small Amplitude Processes in Charged and Neutral One-Component Systems. Phys. Rev., 94:511–525, 1954.

[30] P.J. Dellar. Incompressible limits of lattice Boltzmann equations using multiple relaxation times. Journal of Computational Physics, 190(2):351–370, 2003.

[31] Paul J. Dellar. Nonhydrodynamic modes and *a priori* construction of shallow water lattice Boltzmann equations. Phys. Rev. E, 65:036309, Feb 2002.

[32] C.H. Bruneau and M. Saad. The 2d lid-driven cavity problem revisited. Computers & Fluids, 35(3):326–348, 2006.

[33] SS Chikatamarla, S. Ansumali, and IV Karlin. Grad's approximation for missing data in lattice Boltzmann simulations. EPL (Europhysics Letters), 74:215, 2006.